

1 **The role of polysaccharides and diatom exudates**
2 **in the redox cycling of Fe and the photoproduction of**
3 **hydrogen peroxide in coastal seawaters**

4 Sebastian Steigenberger¹, Peter J. Statham², Christoph Völker¹ and Uta Passow¹

5

6 ¹Alfred Wegener Institut für Polar- und Meeresforschung, Am Handelshafen 12,
7 27570 Bremerhaven, Germany

8 ²National Oceanography Centre, Southampton, University of Southampton Waterfront
9 Campus, European Way, Southampton SO14 3ZH

10

11 **Abstract**

12 The effect of artificial acidic polysaccharides (PS) and exudates of
13 *Phaeodactylum tricorutum* on the half-life of Fe(II) in seawater was investigated in
14 laboratory experiments. Strong photochemical hydrogen peroxide (H₂O₂) production
15 of 5.2 to 10.9 nM (mg C)⁻¹ h⁻¹ was found in the presence of PS and diatom exudates.
16 Furthermore when illuminated with UV light algal exudates kept the concentration of
17 ferrous iron in seawater (initial value 100 nmol L⁻¹) elevated for about 50 min. Since
18 no stabilising effect of PS on Fe(II) in the dark could be detected, enhanced
19 photoreduction seems to be the cause. This was confirmed by a simple model of the
20 photochemical redox cycle of iron. Diatom exudates seem to play an important role
21 for the photochemistry of iron in coastal waters.

22

23 1 Introduction

24 Marine phytoplankton contributes significantly to the CO₂ exchange between
25 atmosphere and ocean, thus impacting atmospheric CO₂ concentrations (Falkowski *et*
26 *al.* 1998). Global marine primary productivity shows great spatial and temporal
27 variability, caused primarily by variable light, zooplankton grazing and nutrient
28 distributions. In addition to the macronutrients (P, N), iron is an essential trace
29 element for photo-autotrophic organisms (Geider *et al.* 1994; Falkowski *et al.* 1998;
30 Morel *et al.* 2003). Several large scale iron fertilization experiments have revealed
31 that in 40% of the surface ocean, the so called High Nutrient Low Chlorophyll
32 (HNLC) areas, iron is at least partially responsible for limitation of phytoplankton
33 growth (Boyd *et al.* 2007). However, iron limitation can occur in coastal areas as well
34 (Hutchins *et al.* 1998) and here the supply of Fe through upwelling and resuspension
35 determine its cycling.

36 Free hydrated Fe(III) concentrations in seawater are very low ($<10^{-20}$ mol L⁻¹) (Rue *et*
37 *al.* 1995) and the more soluble Fe(II) is rapidly oxidised (Millero *et al.* 1987; Millero
38 *et al.* 1989; King *et al.* 1995; Gonzalez-Davila *et al.* 2005, 2006). Thus concentrations
39 of dissolved Fe in the ocean should be very low. However, over 99% of the dissolved
40 iron in seawater is reported to be bound by organic compounds (Rue *et al.* 1995; van
41 den Berg 1995; Croot *et al.* 2000; Boye 2001) and these ligands can maintain the
42 concentrations typically seen in the ocean (Johnson *et al.* 1997). Iron binding ligands
43 in seawater mainly consist of bacterial siderophores (Macrellis *et al.* 2001; Butler
44 2005) and possibly planktonic exudates like acidic polysaccharides (PS) (Tanaka *et*
45 *al.* 1971). Transparent exopolymer particles (TEP), which are rich in acidic

46 polysaccharides, are ubiquitous in the surface ocean (Passow 2002). TEP has been
47 shown to bind ²³⁴Th (Passow *et al.* 2006) and are therefore a prime candidate to bind
48 iron.

49 The main oxidation pathway of Fe(II) to Fe(III) is the reaction with O₂ and
50 H₂O₂ according to the Haber-Weiss mechanism (Millero *et al.* 1987; Millero *et al.*
51 1989; King *et al.* 1995). This oxidation can be inhibited (Theis *et al.* 1974; Miles *et*
52 *al.* 1981) or accelerated (Sedlak *et al.* 1993; Rose *et al.* 2002, 2003a) in the presence
53 of organic compounds. The decrease in apparent oxidation rate is suggested to be due
54 to stronger photoreduction of Fe(III) (Kuma *et al.* 1995) or stabilisation of Fe(II)
55 (Santana-Casiano *et al.* 2000; Rose *et al.* 2003b; Santana-Casiano *et al.* 2004).

56 In marine systems H₂O₂ functions as a strong oxidant or a reductant (Millero
57 *et al.* 1989; Croot *et al.* 2005). Thus it is important for the cycling of organic
58 compounds and trace metals like Fe (Millero *et al.* 1989). H₂O₂ is the most stable
59 intermediate in the reduction of O₂ to H₂O and is mainly produced in the water
60 column by photochemical reactions involving dissolved organic matter (DOM) and
61 O₂ (Cooper *et al.* 1988; Scully *et al.* 1996; Yocis *et al.* 2000; Yuan *et al.* 2001). Light
62 absorbed by DOM induces an electron transfer to molecular oxygen, forming the
63 superoxide anion radical, which undergoes disproportionation to form hydrogen
64 peroxide. Hence light, O₂, H₂O₂ and organic compounds are important factors in the
65 very complex chemistry of iron in seawater.

66 Increased photochemical reduction of Fe(III) in the presence of sugar acids has
67 been reported (Kuma *et al.* 1992; Ozturk *et al.* 2004; Rijkenberg *et al.* 2005) but for
68 polysaccharides no such studies have been carried out so far. However, the relative
69 abundance of polysaccharides in marine dissolved organic matter (DOM) is about

70 50% (Benner *et al.* 1992) and in phytoplankton derived DOM the fraction of
71 polysaccharides can be up to 64% (Hellebust 1965; Hellebust 1974). In the study
72 reported here we investigate the effect of PS and algal exudates on the photochemical
73 redox cycle of iron and production of H₂O₂.

74

75 **2 Materials and Methods**

76 *2.1 General*

77 Three different types of experiments were conducted to investigate the effect
78 of PS and diatom exudates in combination with UV light on the speciation of iron and
79 the production of H₂O₂. All experiments were conducted at a constant temperature
80 (about 20°C) in the laboratory. In experiments 1 and 3 were samples were exposed to
81 UV radiation, UV transparent 3 L Tedlar bags were used as incubation containers.
82 Experiment 2 was conducted in 30 mL polystyrene screw cap tubes, without UV
83 irradiation.

84 The natural coastal seawater (SW) was collected in July 2006 off Lepe near
85 Southampton (UK), filtered through 0.2 µm membranes and stored at 5°C. Organic
86 matter was removed from a part of this SW via photo-oxidation with strong UV
87 radiation. The so called “organic-free” UVSW (Donat *et al.* 1988) was also stored at
88 5°C.

89 We used gum xanthan, laminarin and carrageenan (all from Sigma) as the
90 artificial PSs. The molecular weight of laminarin is 7700 g mol⁻¹ (Rice *et al.* 2004)
91 and 43% (w/w) of the molecule is carbon. For gum xanthan and carrageenan no
92 specifications could be found but we assumed a carbon content of ~40% (w/w).

93 Diatom exudates were collected as the 0.4 μm filtrate of a senescent culture of
94 *Phaeodactylum tricornerutum* grown in f/2 medium. Ford and Percival (1965) separated
95 a significant amount of a water-soluble glucan from an aqueous extract of
96 *Phaeodactylum tricornerutum*, and their results showed this polysaccharide to be a
97 typical chrysolaminarin with essential similar properties to the p-1,3-linked glucan,
98 laminarin.

99 Philips 40TL12 and Philips 40T'05 lamps, respectively, were used as a light
100 source for the irradiation of samples with UVB and UVA light during experiments 1
101 and 3. Irradiance was measured with a UVA (315-400 nm) sensor type 2.5, a UVB
102 (280-315 nm) sensor type 1.5 (INDIUM-SENSOR, Germany) and a spherical
103 quantum sensor SPQA 2651 (LI-COR) for the photosynthetically active radiation
104 (PAR, 400-700 nm). Sensors were coupled to a data logger LI-1400 (LI-COR). The
105 following irradiance values were used for all light incubations during this study:
106 UVB=0.3 W m^{-2} , UVA=17.6 W m^{-2} and PAR=3.8 W m^{-2} . For all experiments
107 samples were held in UV transparent 3 L polyvinyl fluoride (PVF, Tedlar) bags (SKC
108 Inc., USA), fitted with a polypropylene hose for filling and sub-sampling.

109

110 2.2 Specific Experiments

111 2.2.1 *Experiment 1: Effect of polysaccharides on the photogeneration of H_2O_2*

112 Four pairs of Tedlar bags were filled with MQ water and concentrated
113 solutions of three different PSs were added to three pairs of these bags. For this
114 experiment carrageenan, gum xanthan and laminarin were used. The PSs were
115 dissolved in MQ water by sonicating for 30 min. The final concentration of PS was

116 10 mg L⁻¹ in about 2.3 L. The last pair of bags served as control and contained no PS.
117 One bag of each pair was placed in the dark the other was illuminated with UV light
118 for 270 min. H₂O₂ was measured 1 h before illumination and after 0, 10, 30, 90,
119 270 min in the light and the dark sample.

120

121 2.2.2 *Experiment 2: Effect of polysaccharides on the oxidation of Fe(II) in seawater* 122 *in the dark*

123 Ten clean polystyrene screw cap tubes (30 mL) were filled with the natural
124 Solent seawater (0.2 µm filtered) and another ten tubes were filled with the organic-
125 free Solent Seawater. To 5 tubes of each treatment gum xanthan was added to a final
126 concentration of 1 mg L⁻¹ and the samples were sonicated for 30 min. Initially Fe(II)
127 equivalent to 200 nmol L⁻¹ was added to all tubes, and Fe(II) and H₂O₂ measured after
128 0, 2, 6, 18, 54 min. Temperature, salinity, oxygen concentration and pH were
129 measured before the iron addition and at the end of the experiment.

130

131 2.2.3 *Experiment 3: Effect of diatom exudates and UVA/B radiation on the oxidation* 132 *of Fe(II) in seawater*

133 Three Tedlar bags were filled with about 1 L of organic-free seawater (0.2 µm
134 filtered). One bag served as a control and no further additions were made. To the
135 second bag 100 nmol L⁻¹ Fe(II) were added. To the third bag an addition of diatom
136 exudates and 100 nmol L⁻¹ Fe(II) was made. The amount of diatom exudates added to
137 the sample was chosen in order to reach a concentration of PS similar to natural
138 Solent seawater (0.4 mg glucose eq. L⁻¹). Ferrous iron concentration was measured

139 over a 60 min period after the iron addition. The UV light was switched on for the
140 whole experiment right after the addition of iron to the sample bags. Temperature,
141 salinity, oxygen concentration, pH and total iron were measured before the iron
142 addition and at the end of the experiment. H_2O_2 in the organic-free seawater was
143 adjusted to an initial concentration of 5 nmol L^{-1} and was measured again at the end of
144 the experiment.

145

146 2.3 Analyses

147 Iron concentrations in the samples were determined using a colorimetric
148 method described by Stookey (1970) and Viollier *et al.* (2000). Briefly Ferrozine (the
149 disodium salt of 3-(2-pyridyl)-5,6-bis(4-phenylsulfonic acid)-1,2,4-triazine) forms a
150 magenta coloured tris complex with ferrous iron. The water soluble complex is stable
151 and quantitatively formed in a few minutes at $\text{pH} = 4-9$ after adding an aqueous
152 0.01 mol L^{-1} Ferrozine solution. The absorbance was measured with a Hitachi U-1500
153 at 562 nm in 10 cm cuvettes buffered with an ammonium acetate buffer adjusted to
154 $\text{pH} = 5.5$, and compared to a calibration curve made by standard additions to the
155 sample water. Standards were prepared from a 10 mmol L^{-1} Fe(II) stock solution
156 ($\text{Fe}(\text{NH}_4)_2(\text{SO}_4)_2 \cdot 6\text{H}_2\text{O}$ in 0.1 mol L^{-1} HCl) diluted in 0.01 mol L^{-1} HCl. Total iron
157 was determined by previous reduction of the iron present in the sample under acid
158 conditions over 2 h at room temperature by adding hydroxylamine hydrochloride
159 (1.4 mol L^{-1} in 5 mol L^{-1} HCl) as the reducing agent. The detection limit of this
160 method is about 8 nmol L^{-1} of Fe(II) and the standard error is about 20%. All
161 Reagents were from Sigma-Aldrich and at least p.a. grade. All solutions were
162 prepared in MQ water ($18 \text{ M}\Omega \text{ cm}^{-1}$) purified with a Millipore deionisation system.

163 Samples were prepared in 30 mL polystyrene screw cap tubes. All equipment has
164 been carefully acid washed prior to use.

165 Concentrations of dissolved mono- and polysaccharides were determined semi
166 quantitatively using another colorimetric method described by Myklestad *et al.*
167 (1997). Briefly the absorbance of the strong coloured complex of 2,4,6-tripyridyl-s-
168 triazine (TPTZ) formed with iron reduced by monosaccharides or previously
169 hydrolyzed polysaccharides at alkaline pH is measured at 595 nm in 2.5 cm cuvettes
170 and compared to a calibration curve prepared from D-glucose in MQ water. Total
171 sugar concentration was determined after hydrolysis of the acidified sample in a
172 sealed glass ampoule at 150°C for 90 min. The detection limit was
173 0.02 mg glucose eq. L⁻¹ and the standard error was about 3%. All glassware and
174 reagents were prepared as described by Myklestad *et al.* (1997).

175 For the determination of hydrogen peroxide (H₂O₂) a chemiluminescence flow
176 injection analysis (FIA-CL) described by Yuan and Shiller (1999) was used. The
177 method is based on oxidation of luminol by hydrogen peroxide in an alkaline solution
178 using Co(II) as a catalyst. Our flow injection system generally resembled that
179 described by Yuan and Shiller (1999) but as a detection unit we used the photosensor
180 module H8443 (Hamamatsu) with a power supply and a signal amplifier. The voltage
181 signal was logged every second using an A/D converter and logging software (PMD-
182 1208LS, Tracer DAQ 1.6.1.0, Measurement Computing Corporation). The
183 chemiluminescence peaks were evaluated by calculating their area. The detection
184 limit was 0.1 nmol L⁻¹ and the standard error was 4%. All reagents and solutions were
185 prepared as described by Yuan and Shiller (1999). Since ferrous iron in the sample
186 shows a significant positive interference (Yuan *et al.* 1999) H₂O₂ was measured in

187 parallel samples without added Fe(II) or after one hour when most of the iron was
188 reoxidised.

189 A WTW 315i T/S system was used to determine temperature and salinity in
190 the sample. Oxygen was measured using a WPA OX20 oxygen meter. The dissolved
191 organic carbon (DOC) content in the 0.2 μm filtered samples was measured with a
192 Shimadzu TOC-VCSN system via high temperature catalytic oxidation (HTCO) on Pt
193 covered Al_2O_3 beads. The detection limit of this method is $\sim 3 \mu\text{mol L}^{-1}$ and the
194 precision is $\pm 2 \mu\text{mol L}^{-1}$.

195 The UV photooxidation system consisted of a fan cooled 1 kW medium
196 pressure mercury lamp (Hanovia), with 10 x 200 mL quartz tubes mounted around the
197 axial lamp. After 6 h of UV irradiation the samples were considered “organic-free”
198 (UVSW) (Donat *et al.* 1988). To remove the resulting high concentrations of H_2O_2 the
199 organic-free water was treated with activated charcoal. The charcoal had previously
200 been washed several times with HCl, ethanol and MQ water to remove contaminants.
201 After stirring for 30-40 min the charcoal was removed by filtration through a 0.2 μm
202 polycarbonate membrane. The H_2O_2 concentration in the resulting water was less than
203 0.5 nmol L^{-1} and no contamination with iron was detectable.

204

205 **3 Results and discussion**

206 **3.1 Experiment 1: Effect of polysaccharides on the photochemical production of** 207 **H_2O_2**

208 The first experiment, examining the effect of polysaccharides on the
209 photochemical production of H_2O_2 , showed that within 270 min (4.5 h) of

210 illumination large amounts ($140\text{-}240\text{ nmol L}^{-1}$) of H_2O_2 were formed due to the
211 addition of 10 mg L^{-1} of polysaccharides to MQ water (Figure 1). The H_2O_2
212 concentrations in all samples increased linearly during the experiment, after the light
213 was switched on. Gum xanthan showed the highest photochemical production of H_2O_2
214 followed by carrageenan and laminarin, which can be explained by their different
215 absorptivity at $<400\text{ nm}$ (Figure 2). The addition of laminarin led to a net
216 accumulation rate of H_2O_2 of $22.5\text{ nmol L}^{-1}\text{ h}^{-1}$, which was twice as high as that for
217 pure MQ water ($12.3\text{ nmol L}^{-1}\text{ h}^{-1}$). The H_2O_2 accumulation during illumination of the
218 MQ water was probably due to organic matter leaching from the resin of the filter
219 cartridge of the MQ system. However, the DOC concentration in MQ water was
220 $\ll 10\text{ }\mu\text{mol L}^{-1}$. H_2O_2 accumulation rates of $36.2\text{ nmol L}^{-1}\text{ h}^{-1}$ and $43.4\text{ nmol L}^{-1}\text{ h}^{-1}$
221 were determined in samples with added carrageenan and gum xanthan, respectively.
222 The photochemical production of H_2O_2 was thus 3-4 times higher in the presence of
223 carrageenan and gum xanthan compared to pure MQ water. Linear H_2O_2
224 accumulation rates of similar magnitude have been reported by Cooper *et al.* (1988)
225 and Miller *et al.* (1995) in natural seawater samples. The main structural differences
226 between the molecules of these three PSs are that laminarin has a linear structure of
227 linked glucose monosaccharide units, carrageenan has sulphur containing groups and
228 gum xanthan has a branched structure incorporating uronic acid groups. The PS
229 concentration used in our experiment is equivalent to about 4 mg L^{-1} organic carbon
230 leading to normalised H_2O_2 generation rates of $5.2\text{ nmol L}^{-1}\text{ (mg C)}^{-1}\text{ h}^{-1}$ (laminarin),
231 $9.1\text{ nmol L}^{-1}\text{ (mg C)}^{-1}\text{ h}^{-1}$ (carrageenan) and $10.9\text{ nmol L}^{-1}\text{ (mg C)}^{-1}\text{ h}^{-1}$ (gum xanthan).
232 These values are up to 29 times higher than the rate of $0.38\text{ nmol L}^{-1}\text{ (mg C)}^{-1}\text{ h}^{-1}$
233 reported by Price *et al.* (1998) for the $>8000\text{ Da}$ fraction of natural DOM in the
234 Western Mediterranean even though the light bulbs used in our study typically

235 produced only 25% of the UVB radiation 39% of UVA and 1% of PAR of the
236 calculated natural irradiance found in midday summer sun in the Mediterranean (Zepp
237 *et al.* 1977). The polysaccharides in our study caused strong photogeneration of H₂O₂
238 even under low light exposure probably due to the absence of removal processes such
239 as enzymatic decomposition of H₂O₂ (Moffett *et al.* 1990). Photochemical production
240 rates of H₂O₂ in the Atlantic Ocean and Antarctic waters are much lower ranging from
241 2.1 to 9.6 nmol L⁻¹ h⁻¹ (Obernosterer 2000; Yocis *et al.* 2000; Yuan *et al.* 2001;
242 Gerringa *et al.* 2004). Gerringa *et al.* (2004) calculated a net production rate of
243 7 nmol L⁻¹ h⁻¹ at irradiance levels of 2.8 (UVB), 43 (UVA) and 346 W m⁻² (VIS/PAR)
244 in 0.2 µm filtered water from the eastern Atlantic close to the Equator. These low
245 rates are presumably due to lower DOC concentrations and higher decay rates due to
246 colloids or enzymatic activity in natural waters (Moffett *et al.* 1990; Petasne *et al.*
247 1997). Our experiments suggest that PSs may have had a significant indirect effect on
248 Fe oxidation due to the enhanced photochemical production of H₂O₂.

249

250 3.2 Experiment 2: Effect of gum xanthan on the oxidation of Fe(II) in the dark

251 Differences in the rate of Fe(II) oxidation due to added gum Xanthan were
252 small, both in the natural SW and the UVSW samples (Figure 3 and 4). However, the
253 oxidation of Fe(II) in the natural SW samples (with or without gum xanthan) (Figure
254 3) was much slower than that in the respective DOM-free UVSW samples (Figure 4).
255 Half-life values and oxidation rates of organic-free seawater can be calculated
256 according to Millero and Sotolongo (1989) and Millero *et al.* (1987). Under our
257 experimental conditions the calculated half-life was 25 s for the ambient H₂O₂
258 concentrations and 82 s under O₂ saturation. These theoretical values can be compared

259 to measured Fe(II) half-life values of 42 s (UVSW) and 35 s (UVSW+PS). The
260 measured values resemble the theoretical values under the ambient H₂O₂ conditions.
261 This indicates that the high H₂O₂ concentration had a stronger oxidising effect on
262 Fe(II) than the dissolved O₂ in the samples.

263 For the natural SW sample the theoretical half-life of 43 s under O₂ saturation
264 does not fit the measured data well. The half-life of Fe(II) in the natural SW sample
265 (Figure 3) was ~17 times (11.9 min) and with PS added ~19 times (13.3 min) longer
266 than theoretical value. The measured data followed the exponential oxidation curve
267 calculated for the low H₂O₂ concentration of these samples whereas the high O₂
268 content seemed to not accelerate the measured oxidation of Fe(II).

269 The DOC content of the natural SW (97 µmol L⁻¹) was almost 10 times higher
270 than of the UVSW. The difference in Fe(II) oxidation between the water types might
271 therefore be due to the stabilisation of Fe(II) against oxidation by natural occurring
272 compounds of the coastal SW (Theis *et al.* 1974; Miles *et al.* 1981; Santana-Casiano
273 *et al.* 2000; Rose *et al.* 2003a; Santana-Casiano *et al.* 2004). These results show that
274 the added gum xanthan was not a good model for natural occurring substances
275 stabilising Fe(II) against oxidation. Initial H₂O₂ concentrations also differed
276 appreciably, with 5 nmol L⁻¹ H₂O₂ in the natural SW sample and 270 nmol L⁻¹ H₂O₂ in
277 the UVSW sample. UV oxidation in UVSW water during removal of natural DOM
278 must have caused the differences in H₂O₂. We calculated Fe(II) oxidation rates due to
279 O₂ and H₂O₂ in our experiment to investigate if the differing rates could have been
280 caused by differing initial H₂O₂ concentrations. From the comparison between our
281 measured and theoretically calculated values we conclude that a strong effect of H₂O₂
282 on the lifetime of Fe(II) was observed but no effect of gum xanthan was found in this

283 experiment conducted without irradiation. The lower initial H₂O₂ concentrations in
284 the natural SW sample (5 nmol L⁻¹ H₂O₂; Figure 3) compared to the UVSW sample
285 (270 nmol L⁻¹ H₂O₂; Figure 4) appears to be the major cause for slower Fe(II)
286 oxidation, suggesting that H₂O₂ mainly control the oxidation of Fe(II).

287

288 3.3 Experiment 3: Effect of diatom exudates and UVA/B radiation on the oxidation
289 of Fe(II) in seawater

290 Initially, the half-lives of Fe(II) in both treatments, those with and without
291 addition of diatom exudates, was quite similar (Figure 5). For the initial 5 min (300 s)
292 a half life of 4.5±0.7 min and 4.0±0.3 min, respectively was determined for Fe(II) in
293 the UVSW without and with added diatom exudates. These values are in the same
294 range as published values (Millero *et al.* 1987; Kuma *et al.* 1995; Croot *et al.* 2002).
295 A remarkable difference between both treatments is clearly visible after about 7 min
296 (420 s) (Figure 5). In the UVSW without exudates the Fe(II) concentration continued
297 decreasing exponentially reaching the detection limit after 20 min, whereas in UVSW
298 with added diatom exudates the Fe(II) concentration remained at about 30 nmol L⁻¹
299 decreasing only very slightly with time. The photochemical effect of the exudates was
300 strong enough to result in a net stabilising effect on Fe(II) after 7 minutes.

301 Differences in H₂O₂ production during the first hour of irradiation were
302 significant between UVSW with and without exudates. In the UVSW sample with
303 added diatom exudates a linear production rate of 33 nmol L⁻¹ h⁻¹ H₂O₂ was
304 determined whereas in pure UVSW the respective rate was only 5 nmol L⁻¹ h⁻¹. The
305 higher production rate of H₂O₂ in the presence of exudates, suggests increased
306 photochemical production of H₂O₂. UVSW without exudates contained 11 μmol L⁻¹

307 DOC and no measurable total MS and PS, whereas UVSW mixed with exudates of
308 *Phaeodactylum tricornutum* contained $\sim 450 \mu\text{mol L}^{-1}$ DOC, including
309 $0.4 \text{ mg glucose eq. L}^{-1}$ (i.e. $13 \mu\text{mol C L}^{-1}$) total MS and PS. The DOC- normalised
310 H_2O_2 generation rate of $6.1 \text{ nmol L}^{-1} (\text{mg C})^{-1} \text{ h}^{-1}$ calculated from UVSW with
311 exudates indicates that laminarin-like diatom exudates (Ford *et al.* 1965)
312 photochemically produce H_2O_2 . However, the high DOC content suggests that there
313 was also other organic matter contributing to the photo-production of H_2O_2 .

314 Figure 6 shows a schematic of that part of the iron cycle relevant for our
315 experiment. In pure UVSW the added Fe(II) was oxidised rapidly, but in the presence
316 of ligands contained in the diatom exudates Fe(II) formed FeL, which in the light was
317 released as Fe(II) and then oxidised. The Fe(II) concentration could thus remain stable
318 as Fe(II) production from FeL balanced Fe(II) oxidation. We used a simple numerical
319 model based on these processes to model the Fe(II) concentration in our experimental
320 system.

321 The model uses a constant photoproduction term $k_{\text{hv}}[\text{FeL}]$ of ferrous iron, and
322 constant oxidation rates with oxygen (k_{O_2}). The oxidation rates with hydrogen
323 peroxide ($k_{\text{H}_2\text{O}_2}$) are assumed to increase linearly with a photoformation rate of
324 $33 \text{ nmol L}^{-1} \text{ h}^{-1}$ as measured in this experiment and initial H_2O_2 concentration are set
325 at 4.6 nmol L^{-1} . The initial Fe(II) concentration $[\text{Fe(II)}_0]$ is set at 100 nmol L^{-1} Fe(II),
326 the amount added in the experiment, and increases in the model by the constant
327 photoreduction of the FeL complex (where L is either EDTA or diatom exudates or a
328 combination of both). The direct photoreduction of inorganic iron colloids and
329 dissolved ferric iron is also possible (Waite *et al.* 1984; Wells *et al.* 1991a; Wells *et*
330 *al.* 1991b; Johnson *et al.* 1994), but rates for these processes are negligibly low. For

331 both processes together we calculated about 0.004 nmol L⁻¹ s⁻¹ of Fe(II) for
 332 100 nmol L⁻¹ Fe(II) added using the rates reported by Johnson et al. (1994). The
 333 model assumes that the concentration of FeL changes only negligibly during the
 334 experiment. As loss processes of Fe(II) we included the oxidation of Fe(II) with O₂
 335 and the oxidation with H₂O₂. The latter depends on the increasing H₂O₂
 336 concentrations during the experiment. Since dissociation and formation of FeL are
 337 relatively slow (Hudson *et al.* 1992) compared to the photoreduction of FeL and the
 338 oxidation of Fe(II) we ignored these processes in the model. The model calculates the
 339 change in Fe(II) concentration over time (equation 1).

$$340 \quad \frac{d[Fe(II)]}{dt} = k_{hv}[FeL] - k_{O_2}[Fe(II)_0] - k_{H_2O_2}[H_2O_2][Fe(II)_0] \quad \text{eq. 1}$$

$$341 \quad [H_2O_2] = 33/3600 * t + 4.6 \quad \text{eq. 2}$$

342 t given in [s], k_{hv} and k_{O_2} in [s⁻¹], $k_{H_2O_2}$ in [L nmol⁻¹ s⁻¹] and all concentrations given in
 343 [nmol L⁻¹].

344 The parameters k_{O_2} , k_{hv} [FeL] and $k_{H_2O_2}$ were estimated by fitting the model to the
 345 observed data, minimizing the root mean squared model-data misfit, scaled by the
 346 assumed variance of the measurements. If the deviations between model and data are
 347 independent and normally distributed, the misfit

$$348 \quad \chi^2 = \sum_i \frac{(d_i - m_i)^2}{\sigma_i^2} \quad \text{eq. 3}$$

349 is a χ^2 variable. In this case we can estimate the posterior probability density function
 350 (pdf) of the model parameters (assuming a uniform prior) by

$$351 \quad pdf(k_{O_2}, k_{hv}[FeL], k_{H_2O_2}) \sim \exp\left(\frac{-\chi^2}{2}\right) \quad \text{eq. 4}$$

352 (see e.g. D.S. Sivia (2006)). The probability function is well approximated by a
353 multidimensional Gaussian distribution with a maximum value for the best estimated
354 set of parameter values. To obtain an estimate of the variance for this maximum
355 likelihood estimate of the parameters, we also need an estimate of the covariance
356 matrix of the parameters at the minimum of χ^2 . This covariance matrix can be
357 estimated as the inverse of the Hessian matrix of χ^2 at the minimum. We can then
358 assume a confidence interval (\pm one standard deviation) for the best estimates of the
359 parameters, which are $k_{O_2} = 6.04e-03 \pm 1.20e-03 \text{ s}^{-1}$, $k_{H_2O_2} = 1.97e-04 \pm 8.59e-05$
360 $\text{L nmol}^{-1} \text{ s}^{-1}$ and $k_{hv}[\text{FeL}] = 0.22 \pm 0.06 \text{ nmol L}^{-1} \text{ s}^{-1}$. With this high photoreduction rate
361 the model fits the measured data very well (Figure 7) but the oxidation rates for
362 oxygen and H_2O_2 are 30% lower and 105% higher, respectively, than rates reported
363 by Millero *et al.* (1987; 1989). Holding the oxidation rates k_{O_2} and $k_{H_2O_2}$ fixed at
364 values calculated for the given experimental conditions (22 °C, S = 34.2, O_2 saturated,
365 pH = 8.1) according to Millero *et al.* (1987; 1989) the model-data misfit becomes
366 somewhat larger and the model requires a slightly higher Fe(II) photoproduction term
367 $k_{hv}[\text{FeL}]$ of about $0.24 \pm 0.01 \text{ nmol L}^{-1} \text{ s}^{-1}$ to fit the measured data (Figure 7). The
368 larger error margins when fitting all three parameters, compared to fitting only the
369 photoreduction rate, is explained by the strong correlation between the estimates of
370 $k_{H_2O_2}$ and of $k_{hv}[\text{FeL}]$, meaning that the data can be represented almost equally well
371 with different combinations of these two parameters.

372 The estimated photoproduction rates of Fe(II) are about 50 times higher than the
373 photoreduction rate of inorganic colloidal and dissolved iron calculated before,
374 independent of whether we assume the oxidation rates by Millero *et al.* (1987, 1989).
375 This indicates high photoreduction of Fe(III) mediated by the added organic material.
376 This high reduction of Fe(III) could have resulted either from direct photoreduction of

377 the FeL or indirectly via light induced (see absorbance spectra Figure 2) formation of
378 superoxide ($\text{DOM} + h\nu \rightarrow \text{DOM}^*$; $\text{DOM}^* + \text{O}_2 \rightarrow \text{DOM}^+ + \text{O}_2^-$; and $\text{Fe(III)} + \text{O}_2^-$
379 $\rightarrow \text{Fe(II)} + \text{O}_2$) and the subsequent reduction of ferric iron (King *et al.* 1995; Voelker
380 *et al.* 1995; Rose *et al.* 2005; Fujii *et al.* 2006; Rose *et al.* 2006; Waite *et al.* 2006;
381 Garg *et al.* 2007b, 2007a).

382 Since the estimated laminarin concentration of $\sim 1 \text{ mg L}^{-1}$ only accounts for
383 $\sim 8\%$ of the DOC content of this sample it is not clear to what extent PS were
384 responsible for the photoreduction during this experiment. Some EDTA
385 (concentration of $\sim 1 \text{ } \mu\text{mol L}^{-1}$) had inadvertently also been added with the diatom
386 exudates, as it was part of the culture media. However, photoreduction of iron from
387 complexes with EDTA seemed to have had only a minor effect. Reported steady state
388 Fe(II) concentrations present under stronger irradiation due to photoreduction of Fe-
389 EDTA complexes are much lower (Sunda *et al.* 2003) than observed in this study.
390 Photo-redox cycling of Fe-EDTA complexes has a larger influence on Fe(III)
391 concentrations than on those of Fe(II) (Sunda *et al.* 2003).

392 Steady state concentrations of photochemical Fe(II) are linearly related to the
393 irradiation energy especially in the UV range (Kuma *et al.* 1995; Rijkenberg *et al.*
394 2005; Rijkenberg *et al.* 2006; Laglera *et al.* 2007). In our study the light intensity was
395 only 25% of the UVB radiation 39% of UVA and 1% of PAR of the calculated natural
396 irradiance in midday summer sun at 40°N (Zepp *et al.* 1977). Therefore under natural
397 coastal conditions, with 4-5 times lower DOC concentrations but a 2.6 to 100 times
398 higher irradiance levels, a photoreductive effect of diatom exudates seems highly
399 probable.

400

401 **4 Conclusions**

402 In this study we investigated the photochemical effect of artificial and natural
403 polysaccharide material in aquatic systems on iron speciation and on the production of
404 H₂O₂. Artificial PS caused high photochemical production of H₂O₂, which acts as a
405 strong oxidant for metals and organic matter on the one hand. On the other hand H₂O₂
406 is formed photochemically via the superoxide intermediate which is capable of
407 reducing Fe(III). We found increased steady state Fe(II) concentrations in illuminated
408 seawater with a high concentration of exudates of *Phaeodactylum tricornutum*. In the
409 dark this effect of artificial PS on ferrous iron was not detectable, suggesting that
410 light-produced superoxide reduces Fe(III) maintaining elevated Fe(II) concentration.
411 In coastal seawater with high content of organic matter originating partly from
412 diatoms a positive effect of the exudates on the bioavailability of iron seems likely.
413 Field studies comparing natural phytoplankton bloom waters with open ocean waters
414 are needed to confirm these photoreduction results and the counteracting effect of
415 H₂O₂ on a daily time scale and as a function of particle size (dissolved, colloidal and
416 particulate fraction).

417

418 **5 Acknowledgments**

419 We thank P. Gooddy for his help in the laboratory at the NOCS (UK)
420 and T. Steinhoff and S. Grobe who measured the DOC in our samples at the IfM-
421 Geomar (Germany). Thanks also to N. McArdle for administrative help during this
422 BIOTRACS Early-Stage Training (EST) Fellowship which was funded by the
423 European Union under the Sixth Framework Marie Curie Actions.

425 **6 References**

- 426 Benner, R., J. D. Pakulski, *et al.* (1992). "Bulk chemical characteristics of dissolved
427 organic matter in the ocean." Science **255**: 1561-1564.
- 428
- 429 Boyd, P. W., T. Jickells, *et al.* (2007). "Mesoscale iron enrichment experiments 1993–
430 2005: synthesis and future directions." Science **315**: 612-617.
- 431
- 432 Boye, M. (2001). "Organic complexation of iron in the Southern Ocean." Deep Sea
433 Research I **48**(6): 1477-1497.
- 434
- 435 Butler, A. (2005). "Marine Siderophores and Microbial Iron Mobilization." BioMetals
436 **18**(4): 369-374.
- 437
- 438 Cooper, W. J., R. G. Zika, *et al.* (1988). "Photochemical formation of H₂O₂ in natural
439 waters exposed to sunlight." Environ. Sci. Technol. **22**: 1156-1160.
- 440
- 441 Croot, P. L. and M. Johansson (2000). "Determination of iron speciation by cathodic
442 stripping voltammetry in seawater using the competing ligand 2-(2-Thiazolylazo)-p-
443 cresol (TAC)." Electroanalysis **12**(8): 565-576.
- 444
- 445 Croot, P. L. and P. Laan (2002). "Continuous shipboard determination of Fe(II) in
446 polar waters using flow injection analysis with chemiluminescence detection."
447 Analytica Chimica Acta **466**: 261-273.
- 448
- 449 Croot, P. L., P. Laan, *et al.* (2005). "Spatial and temporal distribution of Fe(II) and
450 H₂O₂ during EisenEx, an open ocean mesoscale iron enrichment." Mar. Chem. **95**:
451 65-88.
- 452
- 453 Donat, J. R. and K. W. Bruland (1988). "Direct determination of dissolved Cobalt and
454 Nickel in seawater by differential pulse cathodic stripping voltammetry preceded by
455 adsorptive collection of cyclohexane-1,2-dione dioxime complexes." Anal. Chem. **60**:
456 240-244.
- 457
- 458 Falkowski, P. G., R. T. Barber, *et al.* (1998). "Biogeochemical controls and feedbacks
459 on ocean primary production." Science **281**(5374): 200-206.
- 460
- 461 Ford, C. W. and E. Percival (1965). "The carbohydrates of *Phaeodactylum*
462 *tricornutum*." J. Chem. Soc.: 7035-7041.
- 463
- 464 Fujii, M., A. L. Rose, *et al.* (2006). "Superoxide-mediated dissolution of amorphous
465 ferric oxyhydroxide in seawater." Environmental Science & Technology **40**(3): 880-
466 887.
- 467
- 468 Garg, S., A. L. Rose, *et al.* (2007a). "Superoxide-mediated reduction of organically
469 complexed iron(III): Impact of pH and competing cations (Ca²⁺)." Geochimica Et
470 Cosmochimica Acta **71**: 5620-5634.

471
472 Garg, S., A. L. Rose, *et al.* (2007b). "Superoxide mediated reduction of organically
473 complexed Iron(III): Comparison of non-dissociative and dissociative reduction
474 pathways." Environmental Science & Technology **41**(9): 3205-3212.
475
476 Geider, R.J, *et al.* (1994). "The role of iron in phytoplankton photosynthesis and the
477 potential for iron-limitation of primary productivity in the sea." Photosynth. Res. **39**:
478 275-301.
479
480 Gerringa, L. J. A., M. J. A. Rijkenberg, *et al.* (2004). "The influence of solar
481 ultraviolet radiation on the photochemical production of H₂O₂ in the equatorial
482 Atlantic Ocean." J. Sea Res. **51**: 3-10.
483
484 Gonzalez-Davila, M., J. M. Santana-Casiano, *et al.* (2005). "Oxidation of iron (II)
485 nanomolar with H₂O₂ in seawater." Geochimica et Cosmochimica Acta **69**(1): 83-93.
486
487 Gonzalez-Davila, M., J. M. Santana-Casiano, *et al.* (2006). "Competition between O₂
488 and H₂O₂ in the oxidation of Fe(II) in natural waters." Journal of Solution Chemistry
489 **35**(1): 95-111.
490
491 Hellebust, J. A. (1965). "Excretion of some organic compounds by marine
492 phytoplankton." Limnol. Oceanogr. **10**: 192-206.
493
494 Hellebust, J. A. (1974). "Extracellular products. In: W. D. P. Stewart, (Ed.), *Algal*
495 *physiology and biochemistry.*" Blackwell: 838-863.
496
497 Hudson, R.J.M, *et al.* (1992). "Investigations of iron coordination and redox reactions
498 in seawater using ⁵⁹Fe radiometry and ion-pair solvent extraction of amphiphilic iron
499 complexes." Marine Chemistry **38**: 209-235.
500
501 Hutchins, D. A. and K. W. Bruland (1998). "Iron-limited diatom growth and Si:N
502 uptake ratios in a coastal upwelling regime." Nature **393**: 561-564.
503
504 Johnson, K. S., K. H. Coale, *et al.* (1994). "Iron photochemistry in seawater from the
505 equatorial Pacific." Mar. Chem. **46**: 319-334.
506
507 Johnson, K. S., R. M. Gordon, *et al.* (1997). "What controls dissolved iron
508 concentrations in the world ocean?" Marine Chemistry **57**(3 / 4): 137.
509
510 King, D. W., H. A. Lounsbury, *et al.* (1995). "Rates and mechanism of Fe(II)
511 oxidation at nanomolar total iron concentrations." Environ. Sci. Technol. **29**: 818-824.
512
513 Kuma, K., S. Nakabayashi, *et al.* (1995). "Photoreduction of Fe(III) by
514 hydrocarboxylic acids in seawater." Water Research **29**(6): 1559-1569.
515
516 Kuma, K., S. Nakabayashi, *et al.* (1992). "Photoreduction of Fe(III) by dissolved
517 organic substances and existence of Fe(II) in seawater during spring blooms." Mar.
518 Chem. **37**: 15-27.
519

520 Laglera, L. M. and C. M. G. Van den Berg (2007). "Wavelength dependence of the
521 photochemical reduction of iron in arctic seawater." Environ. Sci. Technol. **41**: 2296-
522 2302.

523

524 Macrellis, H. M., C. G. Trick, *et al.* (2001). "Collection and detection of natural iron-
525 binding ligands from seawater." Marine Chemistry **76**: 175-187.

526

527 Miles, C. J. and P. L. Brezonik (1981). "Oxygen consumption in humic-colored
528 waters by a photochemical ferrous-ferric catalytic cycle." Environ. Sci. Technol.
529 **15**(9): 1089-1095.

530

531 Miller, W. L., D. W. King, *et al.* (1995). "Photochemical redox cycling of iron in
532 coastal seawater." Mar. Chem. **50**: 63-77.

533

534 Millero, F. J. and S. Sotolongo (1989). "The oxidation of Fe(II) with H₂O₂ in
535 seawater." Geochim. Cosmochim. Acta **53**: 1867-1873.

536

537 Millero, F. J., S. Sotolongo, *et al.* (1987). "The oxidation kinetics of Fe(II) in
538 seawater." Geochim. Cosmochim. Acta **51**: 793-801.

539

540 Moffett, J. W. and O. C. Zafiriou (1990). "An investigation of hydrogen peroxide in
541 surface waters of Vineyard Sound with H₂¹⁸O₂ and ¹⁸O₂." Limnol. Oceanogr. **35**:
542 1221-1229.

543

544 Morel, F. M. M. and N. M. Price (2003). "The biogeochemical cycles of trace metals
545 in the oceans." Science **300**: 944-947.

546

547 Myklestad, S. M., E. Skanoy, *et al.* (1997). "A sensitive and rapid method for analysis
548 of dissolved mono- and polysaccharides in seawater." Marine Chemistry **56**(3-4):
549 279-286.

550

551 Obernosterer, I. B. (2000). "Photochemical transformations of dissolved organic
552 matter and its subsequent utilization by marine bacterioplankton." PhD thesis: 133 pp.

553

554 Ozturk, M., P. L. Croot, *et al.* (2004). "Iron enrichment and photoreduction of iron
555 under UV and PAR in the presence of hydroxycarboxylic acid: implications for
556 phytoplankton growth in the Southern Ocean." Deep Sea Research II **51**: 2841-2856.

557

558 Passow, U. (2002). "Transparent exopolymer particles (TEP) in aquatic
559 environments." Progress in Oceanography **55**: 287-333.

560

561 Passow, U., J. Dunne, *et al.* (2006). "Organic carbon to ²³⁴Th ratios of marine organic
562 matter." Mar. Chem. **100**: 323-336.

563

564 Petasne, R. G. and R. G. Zika (1997). "Hydrogen peroxide lifetimes in south Florida
565 coastal and offshore waters." Mar. Chem. **56**: 215-225.

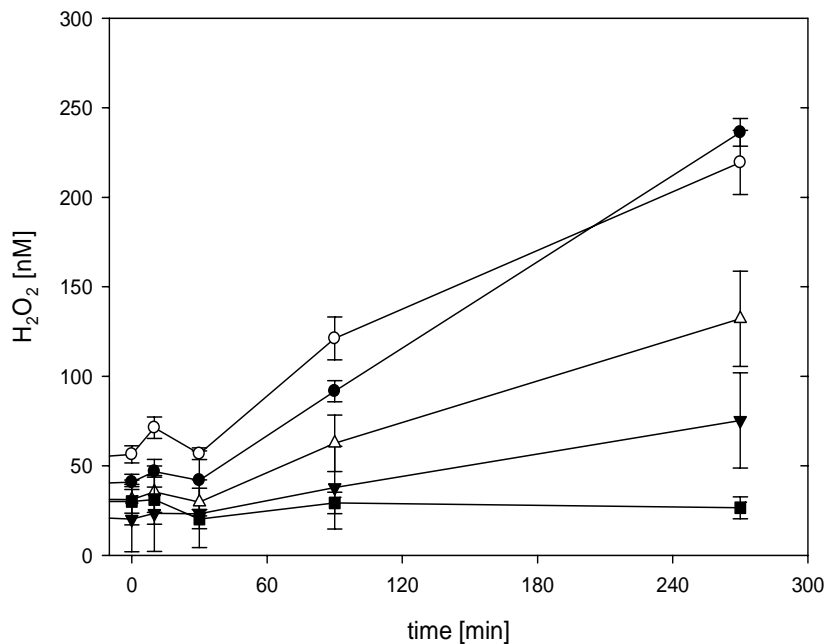
566

567 Price, D., R. F. C. Mantoura, *et al.* (1998). "Shipboard determination of hydrogen
568 peroxide in the western Mediterranean sea using flow injection with
569 chemiluminescence detection." Analytica Chimica Acta **377**: 145-155.

570
571 Rice, P. J., B. E. Lockhart, *et al.* (2004). "Pharmacokinetics of fungal (1–3)- β -Image-
572 glucans following intravenous administration in rats." International
573 Immunopharmacology **4**(9): 1209-1215.
574
575 Rijkenberg, M. J. A., A. C. Fischer, *et al.* (2005). "The influence of UV irradiation on
576 photoreduction of iron in th Southern Ocean." Mar. Chem. **93**: 119-129.
577
578 Rijkenberg, M. J. A., L. J. A. Gerringa, *et al.* (2006). "Enhancement and inhibition of
579 iron photoreduction by individual ligands in open ocean seawater." Geochimica Et
580 Cosmochimica Acta **70**(11): 2790-2805.
581
582 Rose, A. L. and D. Waite (2006). "Role of superoxide in the photochemical reduction
583 of iron in seawater." Geochimica Et Cosmochimica Acta **70**(15): 3869-3882.
584
585 Rose, A. L. and T. D. Waite (2002). "Kinetic model for Fe(II) oxidation in seawater in
586 the absence and presence of natural organic matter." Environ. Sci. Technol. **36**: 433-
587 444.
588
589 Rose, A. L. and T. D. Waite (2003a). "Effect of Dissolved Natural Organic Matter on
590 the Kinetics of Ferrous Iron Oxygenation in Seawater." Environ. Sci. Technol. **37**:
591 4877-4886.
592
593 Rose, A. L. and T. D. Waite (2003b). "Kinetics of iron complexation by dissolved
594 natural organic matter in coastal waters." Marine Chemistry **84**(1-2): 85-103.
595
596 Rose, A. L. and T. D. Waite (2005). "Reduction of organically complexed ferric iron
597 by superoxide in a simulated natural water." Environmental Science & Technology
598 **39**(8): 2645-2650.
599
600 Rue, E. L. and K. W. Bruland (1995). "Complexation of iron(III) by natural organic
601 ligands in the central North Pacific as determined by a new competitive ligand
602 equilibrium / adsorptive cathodic stripping voltammetric method." Marine Chemistry
603 **50**: 117-138.
604
605 Santana-Casiano, J., M. G.-D. Vila, *et al.* (2000). "The effect of organic compounds in
606 the oxidation kinetics of Fe(II)." Marine Chemistry **70**(1-3): 211-222.
607
608 Santana-Casiano, J. M., M. Gonzalez-Davila, *et al.* (2004). "The oxidation of Fe(II) in
609 NaCl-HCO₃⁻ and seawater solutions in the presence of phthalate and salicylate ions: a
610 kinetic model." Mar. Chem. **85**(1-2): 27-40.
611
612 Scully, N. M., D. J. McQueen, *et al.* (1996). "Hydrogen peroxide formation: The
613 interaction of ultraviolet radiation and dissolved organic carbon in lake waters along a
614 43-75 degrees N gradient." Limnol. Oceanogr. **41**(3): 540-548.
615
616 Sedlak, D. L. and J. Hoigne (1993). "The role of copper and oxalate in the redox
617 cycling of iron in atmospheric waters." Atmospheric Environment **27A**(14): 2173-
618 2185.
619

620 Sivia, D. S. (2006). "Data Analysis, A Bayesian Tutorial." 246 pp.
621
622 Stookey, L. L. (1970). "Ferrozine - a new spectrophotometric reagent for iron." Anal.
623 Chem. **42**(7): 779-781.
624
625 Sunda, W. and S. Huntsman (2003). "Effect of pH, light, and temperature on Fe-
626 EDTA chelation and Fe hydrolysis in seawater." Mar. Chem. **84**: 35-47.
627
628 Tanaka, Hurlburt, *et al.* (1971). "Application of Algal Polysaccharides as *in vivo*
629 Binders of Metal Pollutants." Proceedings of the International Seaweed Symposium **7**:
630 602-604.
631
632 Theis, T. L. and P. C. Singer (1974). "Complexation of Iron(II) by organic matter and
633 its effect on Iron(II) oxygenation." Environ. Sci. Technol. **8**: 569-573.
634
635 van den Berg, C. M. G. (1995). "Evidence for organic complexation of iron in
636 seawater." Marine Chemistry **50**: 139-157.
637
638 Viollier, E., P. W. Inglett, *et al.* (2000). "The ferrozine method revisited: Fe(II)/Fe(III)
639 determination in natural waters." Applied Geochemistry **15**(6): 785-790.
640
641 Voelker, B. M. and D. L. Sedlak (1995). "Iron reduction by photoproduced
642 superoxide in seawater." Mar. Chem. **50**: 93-102.
643
644 Waite, T. D. and F. M. M. Morel (1984). "Photoreductive dissolution of colloidal iron
645 oxides in natural waters." Environmental Science & Technology **18**: 860-868.
646
647 Waite, T. D., A. L. Rose, *et al.* (2006). "Superoxide-mediated reduction of ferric iron
648 in natural aquatic systems." Geochimica Et Cosmochimica Acta **70**(18): A681-A681.
649
650 Wells and M. L. a. L.M.~Mayer (1991a). "The photoconversion of colloidal iron
651 oxyhydroxides in seawater." Deep-Sea-Research A **38**: 1379-1395.
652
653 Wells, M., L. Mayer, *et al.* (1991b). "The photolysis of colloidal iron in the oceans."
654 Nature **252**: 248-250.
655
656 Yocis, B. H., D. J. Kieber, *et al.* (2000). "Photochemical production of hydrogen
657 peroxide in Antarctic Waters." Deep Sea Research I **47**(6): 1077-1099.
658
659 Yuan, J. and A. M. Shiller (1999). "Determination of subnanomolar levels of
660 hydrogen peroxide in seawater by reagent-injection chemiluminescence detection."
661 Analytical Chemistry **71**(10): 1975-1980.
662
663 Yuan, J. and A. M. Shiller (2001). "The distribution of hydrogen peroxide in the
664 southern and central Atlantic ocean." Deep Sea Research II **48**: 2947-2970.
665
666 Zepp, R. G. and D. M. Cline (1977). "Rates of direct photolysis in aquatic
667 environment." Environ. Sci. Technol. **11**(4): 359-366.
668

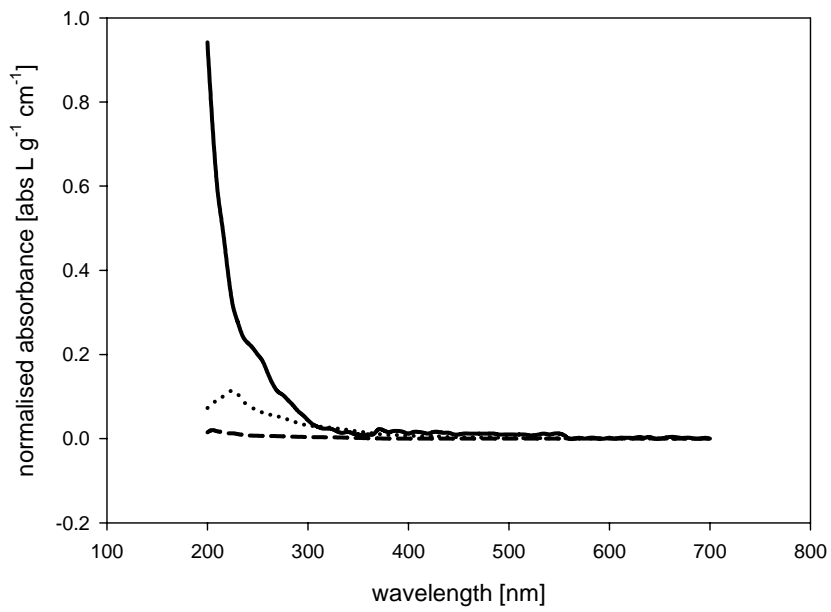
669 7 Figures



670

671 Figure 1: Photogeneration of H₂O₂ during 270 min of irradiation of a 10 mg L⁻¹
672 solution of laminarin (open triangle), carrageenan (open circle), gum xanthan (filled
673 circle) and of pure MQ water (filled triangle) and the mean of all 4 dark controls
674 (filled squares)

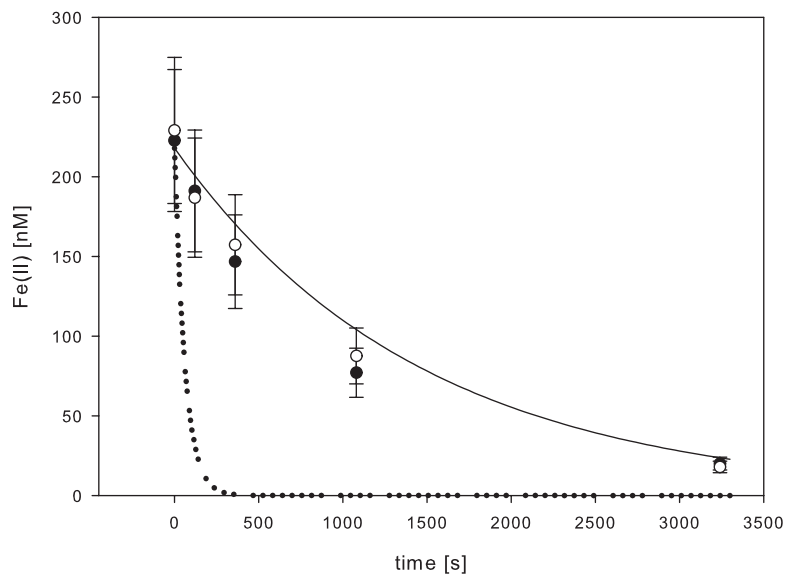
675



676

677 Figure 2: Absorbance spectra (normalised absorbance for 1 g L^{-1} and 5 cm cuvette) of
 678 laminarin (dashed line), carrageenan (dotted line), gum xanthan (solid line) dissolved
 679 in MQ water and filtered over $0.2 \mu\text{m}$ membrane

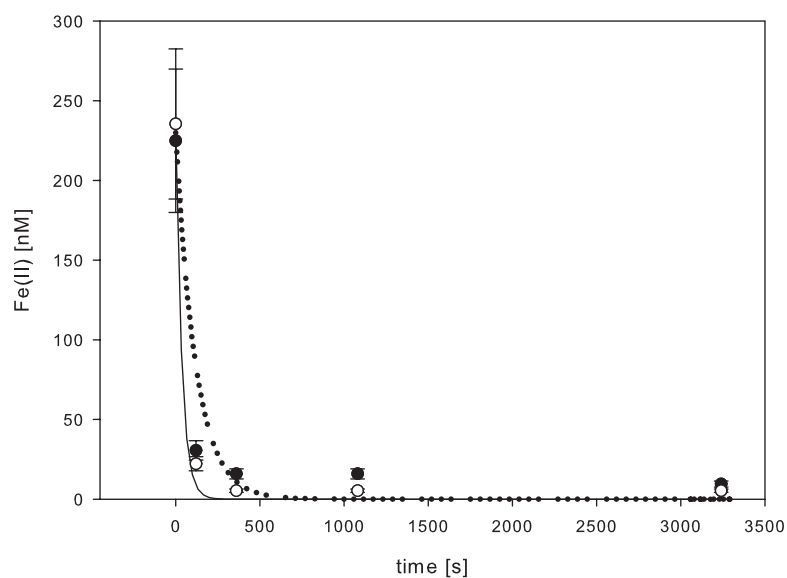
680



681

682 Figure 3: Dark oxidation of 218 nmol L⁻¹ Fe(II) in natural SW (filled circles) and
683 natural SW with PS added. Model results of oxidation of Fe (II) under O₂ saturation
684 (dotted line) and in the presence of 5 nmol L⁻¹ H₂O₂ (solid line) at pH = 8.4, S = 34.1,
685 18 °C are also depicted

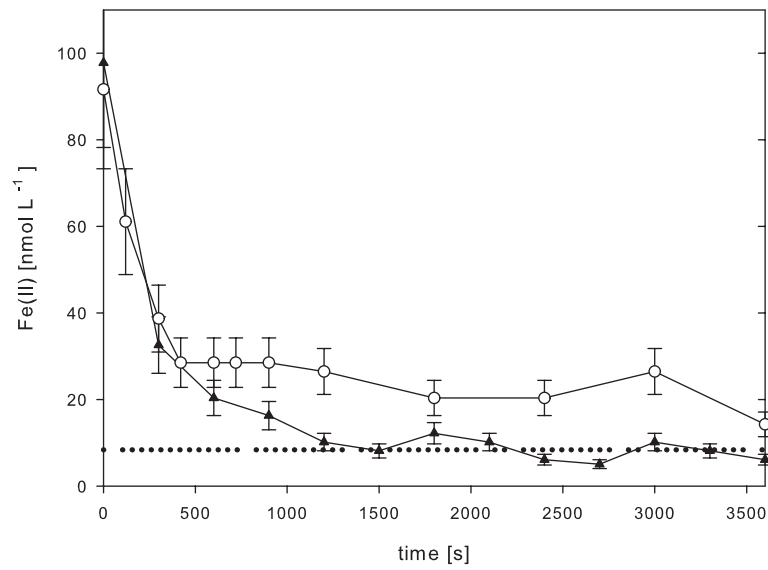
686



687

688 Figure 4: Dark oxidation of 230 nmol L⁻¹ Fe(II) in UVSW (filled circles) and UVSW
689 with PS added. Model results of oxidation of Fe (II) under O₂ saturation (dotted line)
690 and in the presence of 270 nmol L⁻¹ H₂O₂ (solid line) at pH = 8.3, S = 34.1, 17 °C are
691 also depicted

692



693

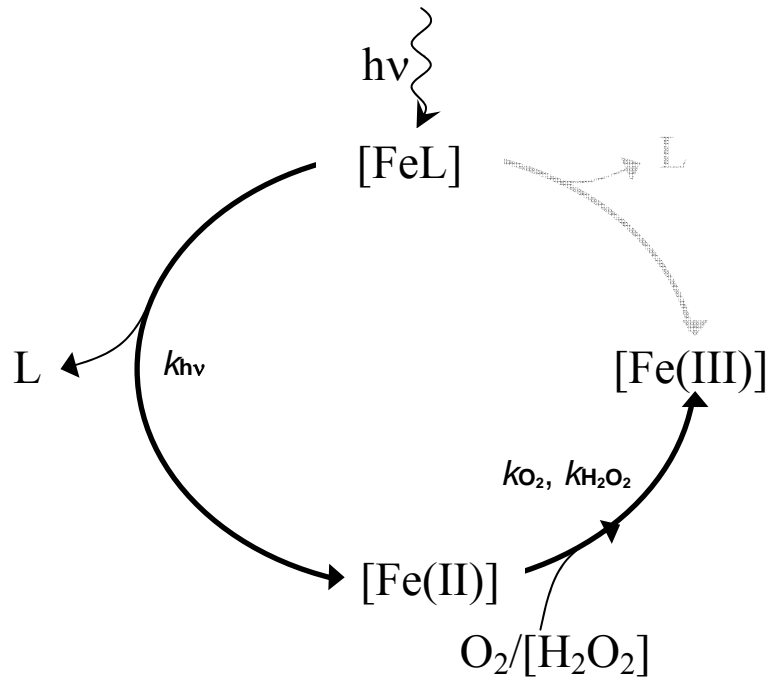
694 Figure 5: Oxidation of Fe(II) in pure UVSW (triangles) and in UVSW with added
 695 diatom exudates (circles) (22 °C, S = 34.2, O₂ saturated, pH = 8.1, UVB = 0.3 W m⁻²,
 696 UVA = 17.6 W m⁻², PAR = 3.8 W m⁻²). The dotted line depicts the detection limit.

697

698

699

700



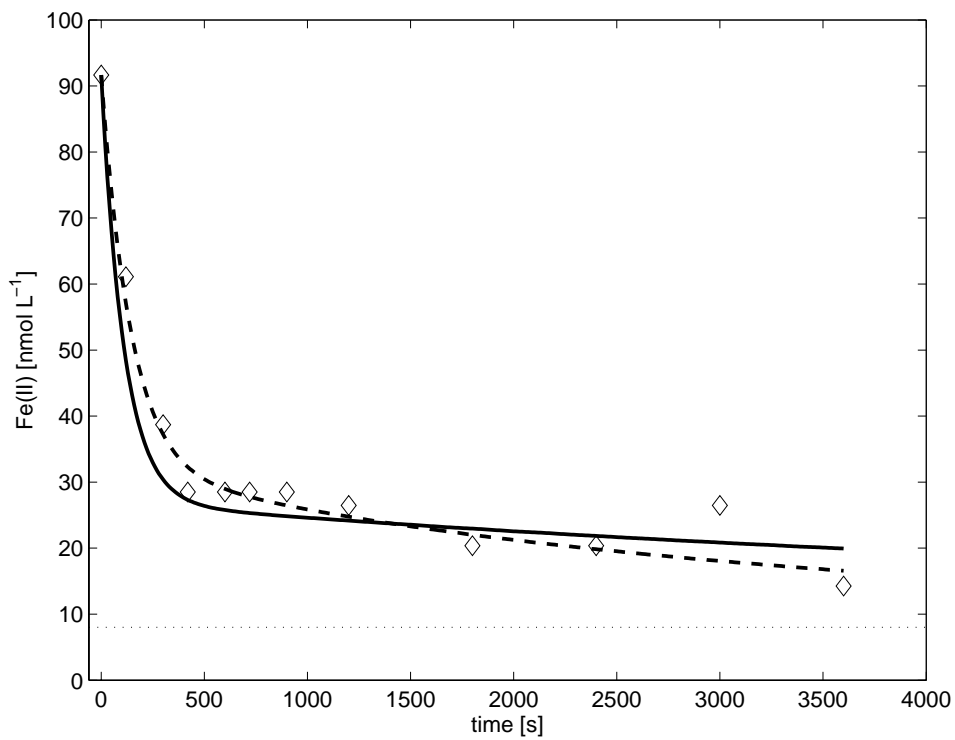
701

702

703 Figure 6: Schematic photoredox cycle for FeL describing the Fe cycling in experiment

704 3 adapted from Sunda and Huntsman (2003)

705



706

707 Figure 7: Best curve fits for measured data (experiment 3) of the oxidation of Fe(II) in
708 UVSW (22 °C, pH = 8.1) with added diatom exudates (diamonds) using fix oxidation
709 rates calculated according to Millero *et al.* (1987; 1989) and the best estimate for the
710 photoproduction term (solid line) and using the best parameter estimates for all three
711 parameters (dashed line) the dotted line shows the detection limit